

## Review Article

# Repurposing proteins for new bioinorganic functions

**Lewis A. Churchfield, Athira George and F. Akif Tezcan**

Department of Chemistry and Biochemistry, University of California, San Diego, La Jolla, CA 92093-0356, U.S.A.

**Correspondence:** F. Akif Tezcan (tezcan@ucsd.edu)

Inspired by the remarkable sophistication and complexity of natural metalloproteins, the field of protein design and engineering has traditionally sought to understand and recapitulate the design principles that underlie the interplay between metals and protein scaffolds. Yet, some recent efforts in the field demonstrate that it is possible to create new metalloproteins with structural, functional and physico-chemical properties that transcend evolutionary boundaries. This essay aims to highlight some of these efforts and draw attention to the ever-expanding scope of bioinorganic chemistry and its new connections to synthetic biology, biotechnology, supramolecular chemistry and materials engineering.

## Introduction

In the broadest sense, the field of bioinorganic chemistry concerns the roles of metal ions in biology, whether as a consequence of natural evolution [1–4] or of human design and intervention [5–7]. Historically, the primary focus of bioinorganic chemistry has been metalloprotein structure and function and the examination of the interplay between metal ions/metallocofactors and protein scaffolds. Proteins are remarkable ligands with immense structural and chemical diversity that offer multiple layers of control over metal reactivity. In return, metal ions modulate protein structure and stability at secondary, tertiary [8] and quaternary levels [9]. All in all, there are slightly more than a handful of metal ions and metallocofactors that are biologically available [3,10,11]. Yet, within the structural context of protein scaffolds, these metal ions and metallocofactors perform a panoply of biological functions and perform challenging biochemical transformations unimaginable in their absence [12,13]. The first detailed glimpses into the synergy between metal ion reactivity and protein scaffolds were provided by the dioxygen-transport proteins haemoglobin and myoglobin, the first two proteins to be structurally characterized by X-ray crystallography [14,15]. Now, five decades later, spurred by advances in structural, spectroscopic, biophysical and analytical characterization, we keep continually being surprised by new ways in which metal–protein synergy takes form. Just a quick scan of the bioinorganic literature from September 2016 reveals: the identification of Cu(I)-binding sites in a human G-protein-coupled receptor protein involved in the olfaction of sulfur-containing odorants [16], the crystal structure of an archaeal 800-kDa formyl-methanofuran dehydrogenase that contains 46 [4Fe–4S] clusters and a 43-Å-long formate diffusion tunnel that couples a CO<sub>2</sub>-reducing tungstopterin site to formyl-methanofuran formation at a dizinc active site [17] and the cryo-EM structural characterization of the entire 1.7-MDa mammalian respirasome architecture, the physiological apparatus responsible for aerobic respiration via numerous redox-active metal centres arranged within multiple protein assemblies [18].

It is difficult not to be awestruck by the sophistication of such bioinorganic machines and resign oneself to the prospect that such sophistication cannot be replicated by design and is best left to analysis. However, one simply needs to realize that nature evolved such machines for functional adequacy and survival, making do with a limited set of available metal ions and metallocofactors and a complete lack of rationality. This realization begets the following question: can the laboratory scientist, equipped with rational thought, knowledge and access to nearly the entire periodic table, surmount the environmental

Received: 01 December 2016  
Revised: 17 January 2017  
Accepted: 23 January 2017Version of Record published:  
9 May 2017

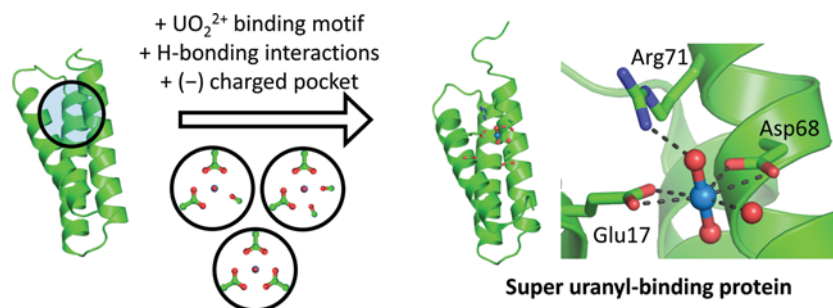


**Figure 1. Engineering a uranyl-binding protein**

A three-helix bundle protein was engineered to accommodate a  $\text{UO}_2^{2+}$  coordination motif with secondary H-bonding interactions and a negatively charged binding pocket. The resulting scaffold, SUP binds  $\text{UO}_2^{2+}$  with femtomolar affinity and very high selectivity over competing metal ions. Adapted with permission from [31]. PDB IDs: 2PMR and 4FZP.

boundaries imposed on living systems and create new metalloproteins with properties that are unprecedented in nature? As this essay aims to illustrate, this can indeed be the case. Although the field of protein design and engineering has historically sought to understand and recapitulate the design principles of natural metalloproteins, some recent efforts in the field have truly broadened the reach of bioinorganic chemistry.

These efforts will be covered under two sections. The first section will highlight work on repurposing the interiors of existing protein scaffolds to widen the functional range of existing metalloproteins or to create entirely novel metal-based functions. The second section will describe the use of proteins as building blocks, wherein their exteriors are redesigned to undergo metal-directed self-assembly into supramolecular architectures with unprecedented structures and emergent properties. The subjects of metalloprotein design and repurposing as well as metal-directed protein self-assembly have been reviewed recently [5–7,19,20]. Thus, our focus here will be on a set of select studies – with emphasis on those from the last 2 years – that have expanded the range of bioinorganic chemistry beyond natural evolution. We refer the readers to the aforementioned review articles and additional works [21–26] for a discussion of many other excellent studies in the field.

## Repurposing protein interiors for new or expanded metal-based functions

The creation of a 3D structural framework is arguably the rate-limiting step in the evolution or design of functional proteins [27,28]. In fact, there are just over a thousand distinct tertiary folding motifs that nature repeatedly uses [11]. A few classic motifs, such as the TIM-barrel, the  $\alpha/\beta$ -hydrolase and the three/four-helix bundle folds are particularly over-represented because they contain mutable elements (loops, pockets, etc.) within stable architectures that can evolve to accommodate different metal ions, metallofactors and substrates. For the same reason, most metalloprotein design and engineering efforts have involved repurposing the interiors of existing protein structures to generate functional diversity, bypassing the need for designing protein folds from scratch [5–7].

## Re-engineering a non-metalloprotein for selective binding of non-biological metal ions

One of the most fundamental bioinorganic functions is the selective binding of metal ions by a protein. The primary thermodynamic determinants of metal binding are the coordinating ligands and the immediate environment surrounding this inner-coordination sphere [8,29,30]. Using a custom algorithm based on geometric parameters of known biological metal coordination motifs and the coordination preferences of the uranyl ion ( $\text{UO}_2^{2+}$ ), He and colleagues have scanned the protein structural database to identify positions within proteins into which  $\text{UO}_2^{2+}$ -binding sites could be installed [31]. For computationally screening initial designs, the researchers considered the following design parameters: (i) equatorial coordination by five to six O-donor atoms furnished by Asp/Asn and Glu/Gln residues at an optimal bond distance of  $\sim 2.5$  Å and (ii) H-bond donors to the axial oxo groups of  $\text{UO}_2^{2+}$  as well as (iii) protein scaffold stability, avoidance of steric clashes and binding site access (Figure 1). From a pool of >12000 structures, the screen led to ten initial designs that provided  $\text{UO}_2^{2+}$  dissociation constants of  $K_d \sim 100$  nM. Based on structural modelling, a three-helix bundle protein of unknown native function was further engineered with negatively charged residues in the secondary coordination sphere (Figure 1). This variant, super uranyl-binding protein

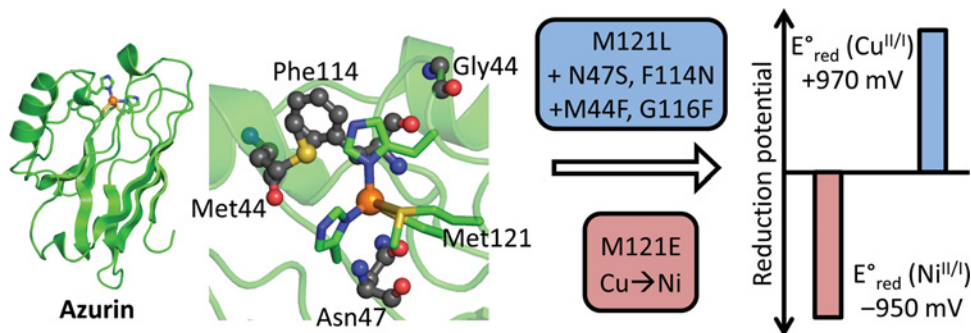


**Figure 2. Modulation of the  $E^{\circ}_{\text{red}}$  of azurin to cover the natural redox spectrum**

The type I Cu centre of azurin can be modified to generate variants with  $E^{\circ}_{\text{red}}$ 's that span the 2-V range observed in nature. Mutating the axial methionine ligand (Met<sup>121</sup>), installing H-bonding interactions and increasing the hydrophobicity of the Cu centre raises  $E^{\circ}_{\text{red}}$  ( $\text{Cu}^{\text{II/I}}$ ) to +970 mV. Mutating Met<sup>121</sup> and substituting the bound Cu for Ni gives a variant with  $E^{\circ}_{\text{red}}(\text{Ni}^{\text{II/I}}) = -950$  mV. Adapted with permission from [34]. PDB ID: 4AZU.

(SUP), bound  $\text{UO}_2^{2+}$  with a femtomolar affinity ( $K_d = 7.4$  fM) and  $>10^4$ -fold selectivity over the relevant metal ions found in seawater, a potential milieu for  $\text{UO}_2^{2+}$  capture. The crystal structure of  $\text{UO}_2^{2+}$ -bound SUP revealed that the desired features of the primary and secondary coordination spheres were largely captured (Figure 1). Importantly, this study introduced an effective strategy for repurposing non-metalloprotein scaffolds towards selective binding of non-biological metal ions to a biologically and technologically useful level.

## Improving the native functions of metalloproteins beyond evolutionary boundaries

Tuning the functional properties of natural metalloproteins beyond the evolutionary limits provides a critical test of our understanding of natural bioinorganic design principles. An important class of metalloproteins is the redox proteins essential in all energy production/transformation processes and numerous biochemical transformations. The key thermodynamic parameter for the execution of redox reactions is the reduction potential ( $E^{\circ}_{\text{red}}$ ) of the active metal centre, which is modulated by the protein fold. In nature,  $E^{\circ}_{\text{red}}$  ranges from approximately +1 V, where water is oxidized to  $\text{O}_2$ , to approximately -1 V, where protons are reduced to  $\text{H}_2$  [32]. Remarkably, biological systems use only three major types of metal centres (Fe-S clusters, haems and Cu centres) to cover the entire 2-V range. Cupredoxins are a large superfamily of proteins that contain type I Cu centres with  $E^{\circ}_{\text{red}}$ 's ( $\text{Cu}^{\text{II/I}}$ ) that span the higher end (100–800 mV) of the physiological redox spectrum. Lu and colleagues asked whether the  $E^{\circ}_{\text{red}}$  of a single cupredoxin, azurin (native  $E^{\circ}_{\text{red}} = 265$  mV) could be tuned across the whole physiological redox range (Figure 2) [33,34]. Rational variation of the axial methionine ligand, adjustment of H-bonding interactions to the Cu ligands and modulation of local hydrophobicity, yielded a range of  $E^{\circ}_{\text{red}}$  (90–970 mV) beyond that of the entire cupredoxin family. Replacement of the Cu centre with Ni uniformly downshifted the  $E^{\circ}_{\text{red}}$  range of the azurin variants, yielding a  $E^{\circ}_{\text{red}}(\text{Ni}^{\text{II/I}})$  range of -950 to 50 mV. Thus, through the modulation of only five amino acid residues and substitution of the metal centre,  $E^{\circ}_{\text{red}}$  of a single metalloprotein was shown to encompass the entire biological redox spectrum, a remarkable demonstration of rational protein redesign.

Another impressive example of augmenting natural metalloprotein function beyond evolutionary limits came from the work of Hilvert and colleagues on the haem enzyme ascorbate peroxidase (APX) [35]. APX uses hydrogen peroxide as an electron acceptor to catalyse the oxidation of organic substrates. In the active site, an aspartic acid residue H-bonds to the proximal histidine ligand of the Fe centre (Figure 3). This interaction is highly conserved among peroxidases and was thought to confer partial imidazolite character to the histidine ligand, thereby increasing electron donation to Fe and facilitating O–O bond heterolysis [36,37]. In order to probe the role of the conserved Asp–His H-bonding, the histidine ligand of an engineered ascorbate peroxidase (APX2) was replaced with an unnatural analogue, *N*-methylhistidine (NMH) [35], which cannot act as an H-donor to aspartic acid and assume the imidazolite state. Surprisingly, it was found that the NMH substituted enzyme (APX2 NMH) was nearly as active as APX2, suggesting that the slightly increased basicity of NMH can compensate for the lack of His–Asp H-bonding. Interestingly, APX2 NMH was remarkably resistant to irreversible inactivation through haem oxidation (a common handicap of

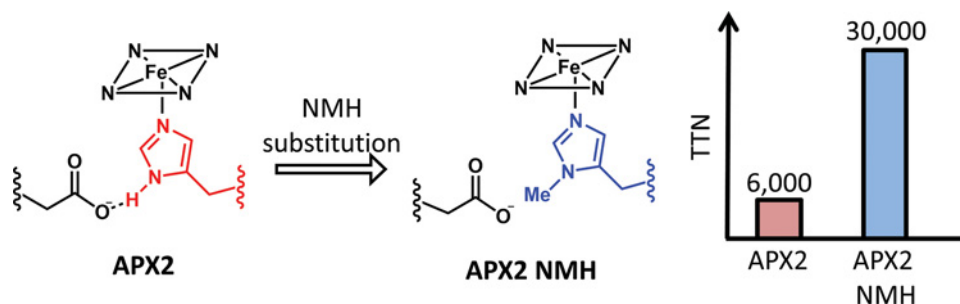


**Figure 3. The enhancement of native APX activity through an unnatural histidine derivative**

Replacing the haem cofactor's axial histidine ligand in APX2 with NMH gives a variant (APX2 NMH) that resists inactivation. Adapted with permission from [35].

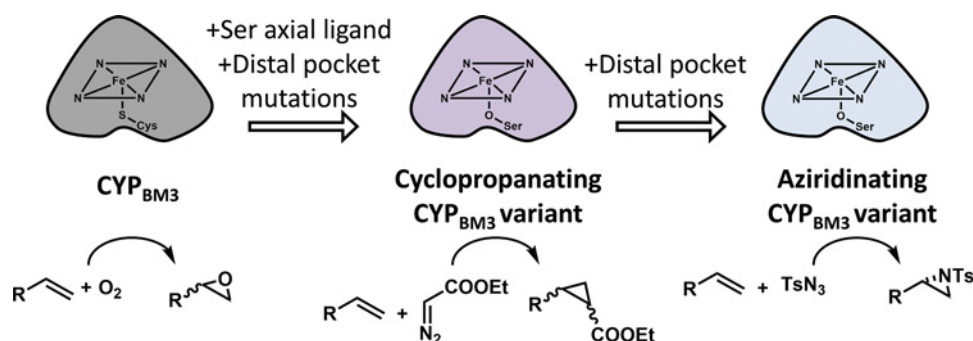


**Figure 4. Repurposing CYP for non-biological catalytic reactions**

The enzyme CYP<sub>BM3</sub> catalyses the epoxidation of alkenes at its haem centre. Mutations to the proximal ligand of the haem and the distal pocket yields a variant that can catalyse the cyclopropanation of alkene substrates. Additional mutations to the distal pocket enable enantioselective aziridination of alkene substrates. For additional details, see [41–43].

peroxidase enzymes) and afforded a total turnover number (TTN) of 30000 compared with 6000 for the parent enzyme (Figure 3). This study not only highlights the utility of non-canonical amino acids in probing structure–function relationships, but also how the performance of evolved metalloenzymes can be dramatically improved by subtle modifications.

## Repurposing proteins for abiological catalytic reactions

The above examples clearly illustrate that there is substantial room for optimizing the native functions of metalloenzymes. Recently, there have also been remarkable developments in the design of artificial metalloenzymes that catalyse chemical reactions that have no precedence in nature [41–44]. Following up on previous work to optimize the performance and stability of enzymes through directed evolution [38–40], Arnold and colleagues have sought to engineer cytochrome P450s (CYPs) – which normally catalyse monooxygenation reactions of organic substrates – towards C–C coupling reactions [41].

In the initial experiments, the researchers established that the haem centre of CYP<sub>BM3</sub> could bind the carbene fragment derived from ethyl diazoacetate (EDA) and catalyse its insertion into olefinic substrates with modest efficiency (TTN = 5); such cyclopropanation reactions have no biological counterpart (Figure 4) [41]. Through screening of previously developed CYP<sub>BM3</sub> mutant libraries and additional point mutations at both the distal haem pocket and the proximal ligand to the Fe-centre, several variants were identified that could not only execute cyclopropanation reactions with great efficiencies (TTN > 67000) and high diastereo/enantioselectivities [42], but also perform nitrene transfer for intramolecular amination and intermolecular aziridination processes (Figure 4) [43]. In further advancement, a haem protein variant was engineered to catalyse C–Si bond formation [44], another transformation not known to occur in biological systems. Screening of several enzymes showed that the *Rhodothermus marinus* cytochrome *c* catalysed the enantioselective coupling of phenyldimethylsilane to ethyl 2-diazopropanoate, albeit with low efficiency

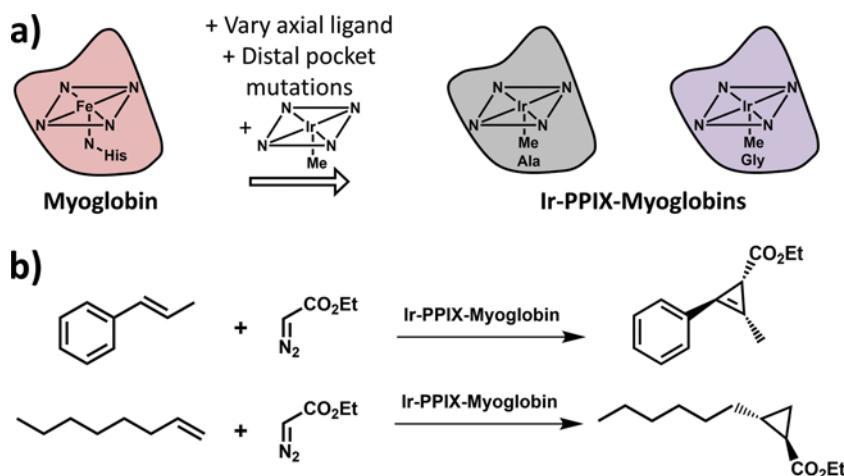


**Figure 5. Incorporation of non-biological metal-porphyrins into myoglobin for non-biological catalysis**

(a) The haem binding pocket of myoglobin can be engineered to accommodate Ir-porphyrins that are active in carbene insertion reactions. (b) Examples of carbene insertion reactions into  $\beta$ -substituted vinylarenes and  $\alpha$ -olefins catalysed by Ir-porphyrin-substituted myoglobin. For additional details, see [50].

(TTN =4) initially. Mutations in the distal haem pocket, including the replacement of the axial Fe-ligand methionine with aspartic acid, afforded a considerably improved variant (TTN >1500) with high enantioselectivity (>99% enantiomeric excess, or ee).

These studies clearly present evidence of the chemical versatility of the haem cofactor, which enables the catalysis of evolutionarily unprecedented C–C, C–N and C–Si coupling reactions when placed in an appropriate protein environment. Yet, as mentioned earlier, nature has at its disposal only a limited number of metallocofactors like the haem, with no facile access to reaction manifolds common to abiological transition metal complexes. This recognition has led to an interest in the reconstitution of protein scaffolds with abiological metal centres in order to couple the rich catalytic chemistry of the latter with the unique advantages of proteins as ligand scaffolds. Although the inception of the field of artificial metallobiocatalysis dates back to 1970s [45,46], the area has burgeoned in recent years. Following the work by Arnold [41–44], Hartwig and colleagues sought to install noble metal–porphyrin complexes, known catalysts for carbene transfer reactions [47–49], within the structural context of myoglobin [50]. The myoglobin scaffold provides a solvent-protected pocket to accommodate various haem derivatives and hydrophobic substrates. In addition, its non-covalently associated, *b*-type haem cofactor can be readily substituted with non-native protoporphyrin IX containing an Ir-methyl centre (Ir-PPIX) both *in vitro* and *in cellulo* (Figure 5a) [50]. Through an extensive screen, Ir-PPIX-myoglobin adducts with the axial histidine mutated to glycine or alanine were established as the most active species for carbene transfer reactions. Subsequently, several amino acid positions lining the distal, substrate-binding pocket were iteratively mutated to create a library of >400 variants. Functional screening of the Ir-PPIX-myoglobin adducts identified variants that catalysed carbene addition to  $\beta$ -substituted vinylarenes and unactivated aliphatic  $\alpha$ -olefins with high enantioselectivities (for either enantiomer) and TTNs, in one case reaching 7200 (Figure 5b). This approach was later extended to a thermostable CYP (CYP<sub>119</sub>) also bearing a *b*-type haem cofactor [51]. In line with the fact that CYP active sites are evolved for the functionalization of organic molecules (as opposed to myoglobin optimized for reversible O<sub>2</sub> binding), the performance of the Ir-PPIX-substituted CYP variants in similar C–C coupling reactions were considerably superior to Ir-PPIX-myoglobin derivatives: up to 98% ee, a TTN of 35000, turnover frequency of 2550 h<sup>-1</sup> and a catalytic efficiency ( $k_{\text{cat}}/K_{\text{m}}$ ) of 260 min<sup>-1</sup> mM<sup>-1</sup>, approximating those of natural enzymes [51].

To host a non-natural metal cofactor, the protein scaffold need not be a native metalloprotein with a preformed active site. In this regard, the robust streptavidin (Sav) scaffold has proven to be particularly versatile, owing to its ability to accommodate a diverse array of organometallic cofactors tethered to a biotin functionality [52], which non-covalently associates with Sav with femtomolar affinity (Figure 6). The result is a highly modular platform where the metalocatalyst and the linker moieties can be synthetically varied and combined with a library of genetically optimized Sav variants that present different microenvironments surrounding the catalyst [52,53]. Based on the Sav-biotin platform, Ward and colleagues have developed an array of artificial metalloenzymes that could execute a number of quintessential organometallic reactions [52], including Ir-catalysed transfer hydrogenation for the reduction of imines



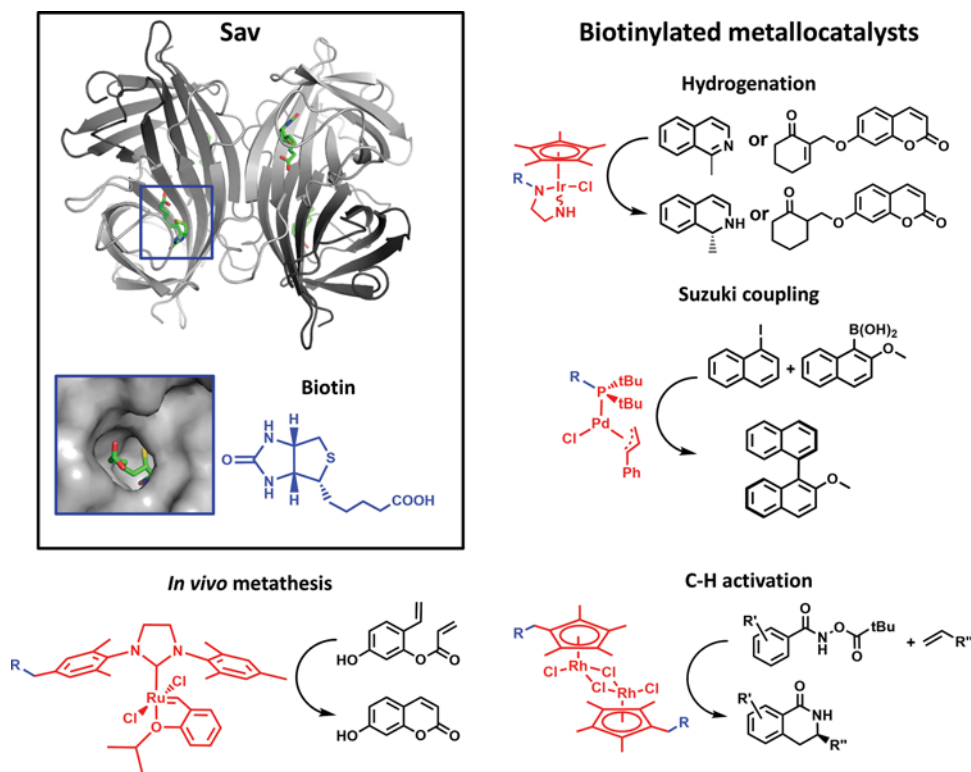


**Figure 6. Creation of artificial metalloenzymes based on the Sav-biotin platform**

The Sav homotetramer tightly binds biotin at a solvent-exposed site. Reactive organometallic moieties can be synthetically linked to biotin and incorporated into Sav to create a modular library of artificial metalloenzymes that are active in many non-biological chemical transformations. PDB ID: 1STP. For additional details, see [52–57].

and enones [54], Pd-mediated Suzuki-coupling reactions [55] and Rh-catalysed C–H activation reactions [56], among others (Figure 6). In all cases, the structural robustness of Sav has allowed for considerable optimization of reaction's enantioselectivity and efficiency, while also providing a protective environment for the organometallic centres, enabling their operation in aqueous media as well as in the presence of other catalysts.

In an exciting advancement, Ward and colleagues demonstrated that their Sav-based metalloenzymes can catalyse abiological reactions within bacterial cells [57]. Towards its end, the researchers designed a Sav variant (Sav<sup>peri</sup>) for expression in the periplasm of *Escherichia coli* cells, a compartment that is reasonably pervious to exogenous molecules. In the periplasm, Sav<sup>peri</sup> could be reconstituted with a biotinylated version of the Hoveyda–Grubbs second-generation Ru-catalyst added to the growth medium (Figure 6). The resulting artificial metalloenzyme biot-Ru-Sav<sup>peri</sup> could catalyse conversion of a non-fluorescent substrate into the fluorescent umbelliferone molecule through ring-closing metathesis (RCM) in living cells. This *in vivo* activity with an optical readout enabled the directed evolution of biot-Ru-Sav<sup>peri</sup> without having to isolate individual protein variants from cell extracts. In turn, this high-throughput screening led to an improved species (biot-Ru-Sav<sup>mut</sup>) with approximately two-fold increase in catalytic efficiency over biot-Ru-Sav<sup>peri</sup> as a result of five mutations surrounding the Ru centre [57]. Impressively, biot-Ru-Sav<sup>mut</sup> outperformed commercially available catalysts in RCM reactions of some water-soluble substrates and its substrate specificity could be further tailored through rational mutagenesis of the active site, for example to accommodate charged substrates.

## Repurposing protein exteriors for the metal-directed self-assembly of functional metalloprotein architectures

The examples above highlight the remarkable functions that can be realized by repurposing the interiors of existing protein folds. However, the scope of small proteins is typically restricted to basic biochemical functions such as binding/recognition, electron transfer and elementary catalytic reactions. On the other hand, nature achieves a much greater structural and functional diversity through the self-assembly of proteins into supramolecular architectures

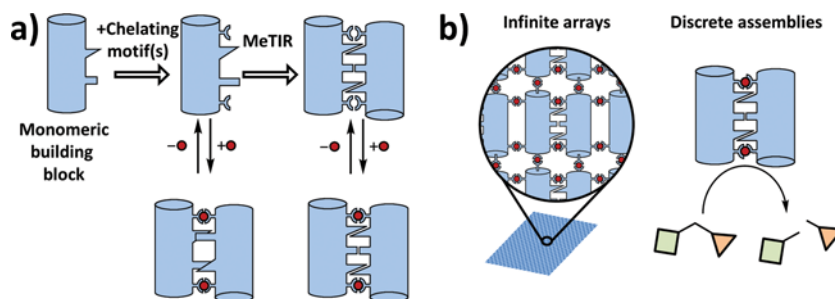


**Figure 7. Metal-directed assembly of proteins into supramolecular architectures**

(a) The exterior of a monomeric protein can be modified by installing chelating motifs that mediate metal-directed self-assembly. Subsequent application of the MeTIR strategy generates self-assembling protein surfaces. (b) Metal-directed protein self-assembly can generate both infinite arrays and discrete assemblies with emergent structural, functional and material properties.

[58]. Indeed, cellular complexity is largely driven by such multimeric protein complexes, which can be categorized into: (i) discrete, oligomeric assemblies (e.g. photosystem II, nitrogenase and cytochrome *c* oxidase) that execute complex, multi-step reactions or (ii) pseudoinfinite polymeric assemblies (e.g. ferritin, microtubules, actin filaments and S-layers) that provide nano/microscale structural materials to sustain the cellular architecture. Protein self-assembly also leads to increased stability, facilitates the engineering of dynamic properties, allostery, stimuli-responsiveness and importantly, generates new molecular interfaces among protein domains that can be used for building new active sites [58–61].

Metal coordination chemistry offers important advantages in terms of constructing protein assemblies that simultaneously possess a targeted structure and function, as well as dynamic and stimuli-responsive properties characteristic of natural protein assemblies [19,20]. Foremost, bonds between (transition) metals and protein-based ligands can be considerably stronger than non-covalent interactions, which obviates the need for designing extensive, non-covalent interfaces for mediating protein self-assembly. Importantly, transition metal ions possess inherent reactivities (e.g. Lewis acidity and redox activity), which are otherwise not readily accessible with amino acid building blocks, thus opening the way to incorporating new inorganic functions into the interfaces of artificial protein assemblies. Finally, metal coordination interactions are innately dependent on environmental stimuli (e.g. pH and redox potential), meaning that the structural/functional properties of metal-directed protein assemblies can be externally controlled. These advantages of metal coordination have been utilized to construct a number of pseudoinfinite and discrete metalloprotein assemblies (Figure 7), thereby adding a new dimension to bioinorganic chemistry. Some recent examples are highlighted below.

## Metal-directed design of periodic/infinite protein assemblies as novel materials

To control protein self-assembly through metal coordination, Tezcan and colleagues installed natural or non-natural bidentate metal-chelating motifs on the surface of a monomeric haem protein (cytochrome *cb*<sub>562</sub> or cyt *cb*<sub>562</sub>) [60,61]. Upon binding late-first-row transition metal ions (Ni<sup>II</sup>, Cu<sup>II</sup>, Zn<sup>II</sup>), the resulting cyt *cb*<sub>562</sub> variants predictably self-assembled into supramolecular complexes whose oligomeric states and symmetries were dictated by the coordination preferences of the metal ions [62]. The propagation of protein self-assembly infinitely in 1D, 2D or 3D requires that the building blocks have at least two different associative surfaces whose relative interaction geometries fulfil certain requirements [63]. Conceptually, this may be achieved through the use of protein building blocks with inherent cyclic (*C*), dihedral (*D*) or cubic (*T* or *O*) symmetries. With this in mind, a computationally redesigned variant of cyt *cb*<sub>562</sub> (RIDC3) was engineered that forms a stable *C*<sub>2</sub> symmetric dimer bearing two coordinatively unsaturated, 3-His ligated Zn ions on its surface (Figure 8a) [64]. The Zn<sub>2</sub>:RIDC3<sub>2</sub> dimer was observed to form crystalline, 2D arrays, which, depending on the metal-controlled nucleation/growth kinetics, could either fold into uniform crystalline, 1D nanotubes or grow into larger 2D and 3D lattices, with dimensions spanning the entire nano–micrometre range (Figure 8a). The 1D and 2D RIDC3 arrays resemble natural assemblies like microtubules and S-layers in terms of their dimensions and structural uniformity, while also recapitulating the ability of these macromolecules to assume distinct conformational states in response to environmental cues such as pH and metal concentrations.

Using protein building blocks of higher symmetries, then, *C*<sub>2</sub> facilitates the design process for metal-directed protein self-assembly and enables additional ways to assert structural control. For example, Brodin et al. [65] engineered

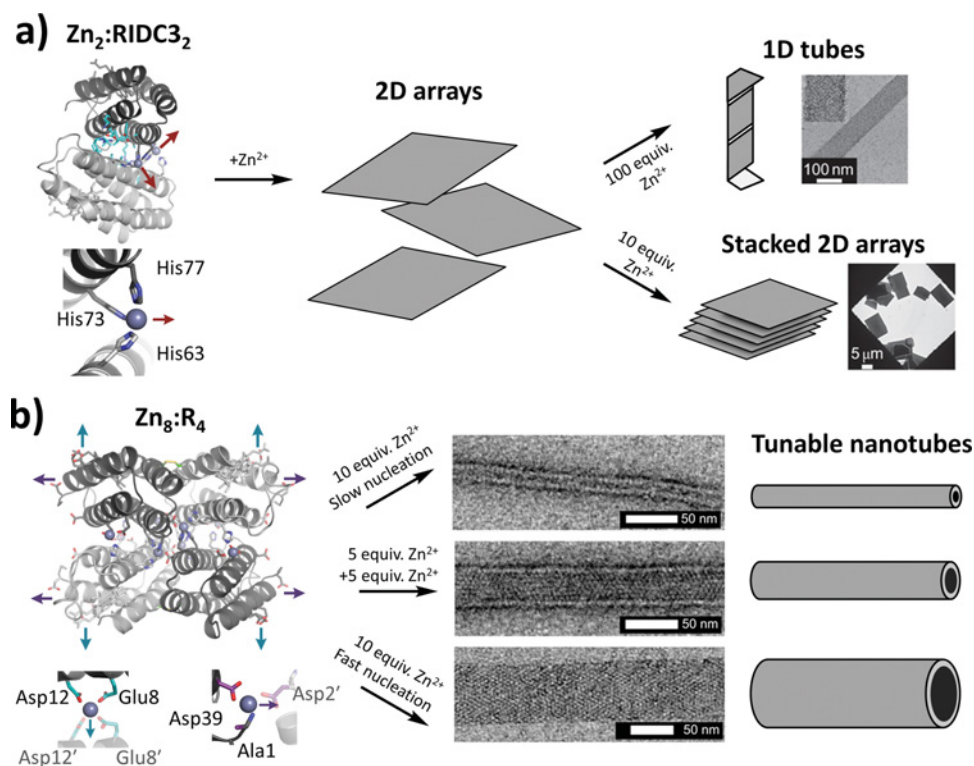


**Figure 8. Metal-directed assembly of 1D and 2D crystalline arrays from *cyt cb*<sub>562</sub> building blocks**

(a) The engineered *cyt cb*<sub>562</sub> variant RIDC3 forms a  $C_2$  symmetric dimer with coordinatively unsaturated Zn-binding sites ( $Zn_2:RIDC3_2$ ). In the presence of excess  $Zn^{II}$ , RIDC3 assembles into 1D tubes or stacked 2D arrays. (b) The  $D_2$  symmetric tetramer,  $Zn_8:R_4$ , possesses two facets that can form intermolecular Zn-binding sites. In the presence of excess  $Zn^{II}$ ,  $Zn_8:R_4$  assembles into nanotubes with tunable diameters. Adapted with permission from [64,65]. PDB IDs: 3TOM and 5BU7.

a stable  $D_2$  symmetric *cyt cb*<sub>562</sub> tetramer ( $Zn_8:R_4$ ) for use as a ‘synthon’ (Figure 8b). The advantage of  $D_2$  symmetry is that it gives rise to two pairs of roughly orthogonal facets on the synthon surface that can be differentially tailored to propagate self-assembly into anisotropic 2D arrays and subsequently into 1D nanotubes of different diameters via metal binding. With  $Zn_8:R_4$ , this was achieved via a pair of bidentate Asp–Glu–dicarboxylate motifs on one pair of facets and a tridentate N-terminal-carboxylate motifs on the second pair of facets. Indeed, by modulating solution conditions (e.g. Zn-to-protein concentration ratios or pH),  $Zn_8:R_4$  assembled into 1D, crystalline nanotubes with controllable diameters and high monodispersity. The physical properties of  $Zn_8:R_4$  nanotubes scaled with their diameters, with the widest nanotubes ( $d = 68 \pm 4$  nm) having a Young’s modulus  $E$  of 0.3 MPa, whereas the narrowest ones ( $d = 20 \pm 2$  nm) possessed an  $E$  of 15 MPa. These values, indicative of stiffness, are comparable to those of natural proteinaceous materials with high flexibilities, such as fibrin networks (1–10 MPa) involved in blood clotting and elastin polymers ( $\sim 1$  MPa) responsible for the elasticity of connective tissue [66]. In  $Zn_8:R_4$  nanotubes, such flexibility and crystalline order are simultaneously attained due to the fact that contacts among the protein building blocks are mediated solely by metal coordination interactions that have a small footprint.

The metal-directed protein design process can be further streamlined by using protein synthons with even higher symmetries. For example, a square-shaped,  $C_4$ -symmetric protein (RhuA) necessitates the incorporation of only two histidine residues in its corners to tessellate into crystalline, 2D lattices upon  $Cu^{II}$  or  $Zn^{II}$  coordination (Figure 9a) [67]. Further, the cube-like,  $O$ -symmetric maxiferritin requires only a single histidine mutation to afford a variant ( $^{H122}$ ferritin) with 3-His coordinated  $Zn^{II}$  ions in its  $C_3$  symmetric pores, corresponding to the eight corners of the ferritin cube (Figure 9b). The metal-bearing corners of ferritin cubes can subsequently be linked through synthetic, ditopic linkers bearing hydroxamate headgroups, producing a 3D, protein–metal–organic framework with the desired body centred cubic lattice arrangement [68].

There are several practical advantages of arranging proteins into crystalline arrays [69]. For instance, both 1D and 2D RIDC3 assemblies display very high stabilities owing to their metal-mediated frameworks, maintaining their



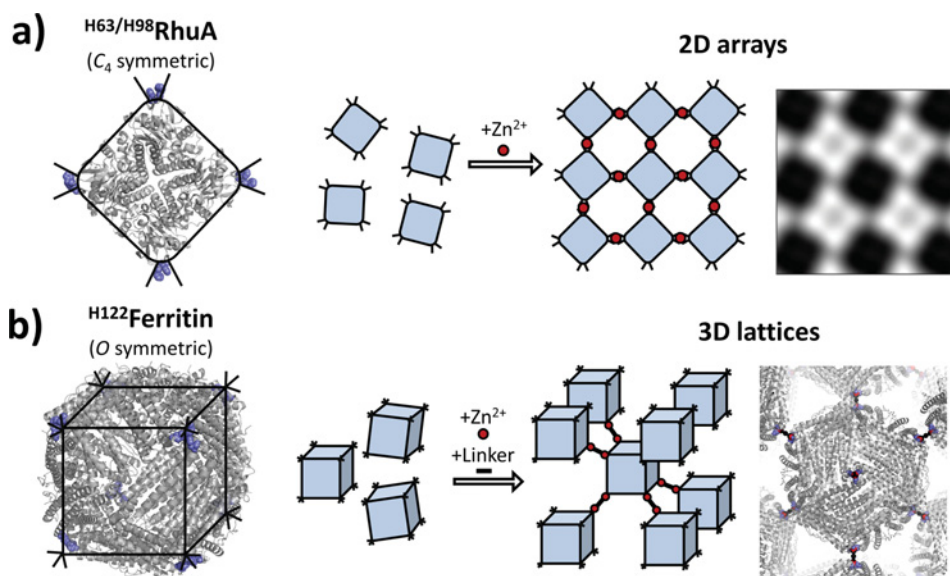


**Figure 9. Assembly of 2D and 3D protein lattices from high-symmetry building blocks**

(a) The C<sub>4</sub>-symmetric H<sub>63</sub>/H<sub>98</sub>RhuA homotetramer, tailored with bis-His motifs in its corners, assembles into 2D crystalline arrays upon metal coordination. (b) The O-symmetric H<sub>122</sub>ferritin cage binds Zn<sup>II</sup> and a di-hydroxamate linker in its three-fold symmetric vertices to form a body centred cubic lattice. Adapted with permission from [67,68]. PDB IDs: 1GT7 and 5CMR.

structural order at up to ~90°C and in ≥90% (v/v) of polar organic solvents including tetrahydrofuran (THF) and propan-2-ol (iPrOH) [69]. In contrast, unassembled RIDC3 monomers denature in ~30% THF and 50% iPrOH. Another advantage protein self-assembly derives from the innate activities of the protein building blocks that can be used to create functional/reactive protein materials. The native function of RIDC3 (or its parent, cyt *b*<sub>562</sub>) is to act as a one-electron transfer shuttle; thus, the supramolecular Zn-RIDC3 arrays represent redox-active nano-templates with high structural periodicity. Brodin et al. used this feature to spatio-temporally control the reductive growth of uniform Pt<sup>0</sup> nanocrystals on the surfaces of 2D Zn-RIDC3 arrays [69]. This emergent functional property was ultimately enabled by both the supramolecular assembly of RIDC3 molecules to form a periodically organized structural template and their haem-based redox activities to direct Pt<sup>II</sup> reduction.

## Metal-directed design of closed/oligomeric protein assemblies with inorganic functions

A structural consequence of metal-directed protein self-assembly is the generation of new protein–protein interfaces around the nucleating metal centres. These evolutionarily ‘naïve’ interfaces, in turn, can be redesigned to tailor the reactivities of the buried metal centres or to endow the supramolecular architecture with new functional properties, a strategy that was termed ‘metal-templated interface redesign’ or MeTIR (Figure 7) [70]. The initial implementations of MeTIR exploited the aforementioned advantages of the D<sub>2</sub> symmetry (three sets of protein–protein interfaces with C<sub>2</sub> symmetry, large interfacial surface area) of a Zn-templated, tetrameric assembly of cyt *cb*<sub>562</sub> variant, Zn<sub>4</sub>:MBPC1<sub>4</sub>. First, computationally prescribed hydrophobic residues were installed on to each monomer to stabilize one set of the interfaces [70], which was followed by incorporation of cysteine residues to form disulfide bonds (Cys<sup>96</sup>–Cys<sup>96′</sup>) across a second one upon self-assembly [71]. The resulting variant C<sup>96</sup>RIDC1 formed a highly stable tetrameric assembly (C<sup>96</sup>RIDC1<sub>4</sub>) even in the absence of metal ions. Excitingly, this assembly bound Zn<sup>II</sup> ions with very high affinity and selectivity over all tested divalent metal ions (including Cu<sup>II</sup>) as intended by the templating strategy [71].

Churchfield et al. [72] recently investigated whether additional disulfide bonds can be built into the interfaces of C<sup>96</sup>RIDC1<sub>4</sub> with the idea that this would: (i) increase the overall rigidity and preorganization of the quaternary assembly around the templating Zn<sup>II</sup> ions and (ii) amplify the overall strain that Zn<sup>II</sup> coordination and the interfacial interactions exert on one another [72]. The latter, in turn, could result in a spring-loaded quaternary structure that could allow structural coupling between the Zn-binding and the disulfide bond formation equilibria. Indeed, a new variant with two additional surface cysteine residues, C<sup>38</sup>/C<sup>81</sup>/C<sup>96</sup>RIDC1, properly self-assembled into a monolithic assembly (Zn<sub>4</sub>:C<sup>38</sup>/C<sup>81</sup>/C<sup>96</sup>RIDC1<sub>4</sub>) bearing disulfide bonds across all three pairs of interfaces. While C<sup>38</sup>/C<sup>81</sup>/C<sup>96</sup>RIDC1<sub>4</sub>

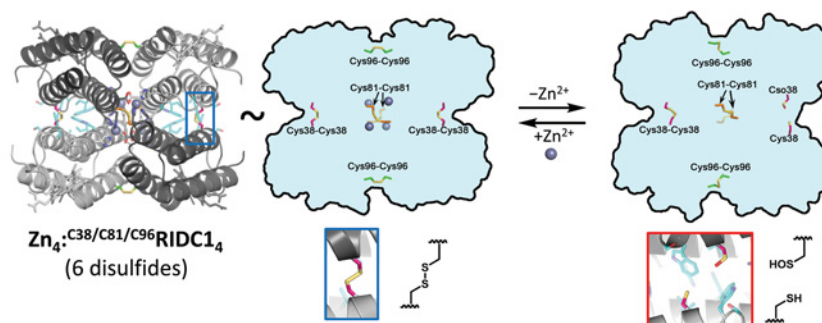


**Figure 10. A *de novo* designed allosteric metalloprotein assembly with strained disulfide bonds**

Following the MeTIR strategy, the insertion of multiple disulfide bonds into the interfaces of a Zn-templated cyt *cb*<sub>562</sub> tetramer creates a highly strained quaternary architecture (Zn<sub>4</sub>:<sup>C38/C81/C96</sup>R1<sub>4</sub>). The quaternary strain enables allosteric coupling between Zn binding by the tetramers and the formation/breakage of a single disulfide bond. Adapted with permission from [75]. PDB ID: 5L32.

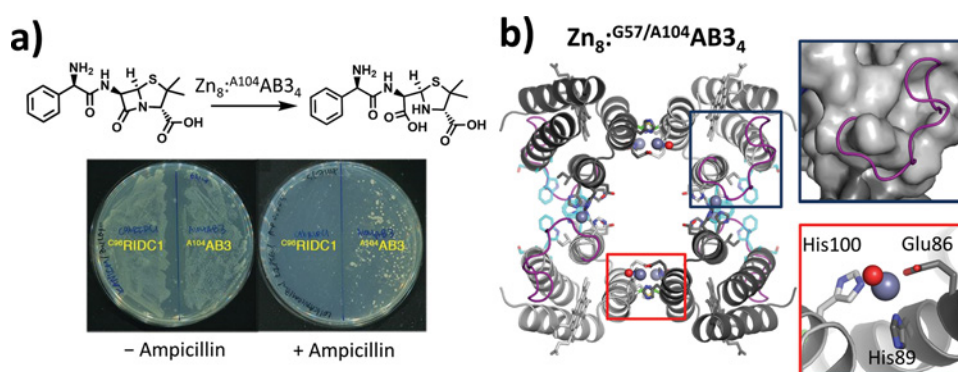


**Figure 11. Design of a supramolecular metalloenzyme assembly with *in vivo* enzymatic activity**

(a) *In vivo* screening/selection of Zn<sub>8</sub>:<sup>G57/A104</sup>AB<sub>3</sub><sub>4</sub> activity through antibiotic resistance enabled by ampicillin hydrolysis. (b) A combination of MeTIR and directed evolution is employed to generate a multimetallic cyt *cb*<sub>562</sub> assembly (Zn<sub>8</sub>:<sup>G57/A104</sup>AB<sub>3</sub><sub>4</sub>) that can catalyse the hydrolysis of activated esters and β-lactam moieties. Adapted with permission from [73]. PDB ID: 4U9E.

still bound four Zn<sup>II</sup> ions, the resulting quaternary strain was reflected in a lowered binding affinity (by ~20 kJ/mol) compared with the unstrained <sup>C96</sup>RIDC1<sub>4</sub>. Notably, the crystal structures of the Zn-bound and apo-<sup>C38/C81/C96</sup>RIDC1<sub>4</sub> showed that, upon Zn-removal, the interfaces underwent considerable conformational changes and one of the six disulfide bonds (Cys<sup>38</sup>–Cys<sup>38'</sup>) dissociated to relieve the quaternary strain (Figure 10). Thus, the increased strain through interfacial redesign allowed metal coordination to be directly and remotely linked to the formation/breakage of a distinct disulfide bond within the quaternary scaffold, thereby creating the first allosteric protein system designed from scratch.

Again using the <sup>C96</sup>RIDC1<sub>4</sub> assembly as the starting point, Song and Tezcan [73] sought to create a catalytic assembly (Figure 11). To this end, four symmetry related, His/His/Asp coordination motifs were incorporated into the *i2* interfaces to create tripodal Zn<sup>II</sup>–OH<sup>−</sup>/OH<sub>2</sub> motifs that resemble the active sites of Zn-hydrolase enzymes. Four Zn<sup>II</sup> sites that nucleated the tetrameric assembly were kept intact to stabilize the quaternary architecture. The crystal structure of the resulting assembly (Zn<sub>8</sub>:AB<sub>3</sub><sub>4</sub>) confirmed the formation of the intended architecture with four internal (structural) and four peripheral (catalytic) Zn-coordination sites, with the exception that the peripheral Zn ions were coordinately saturated by the unforeseen participation of a lysine residue. The substitution of this lysine residue with alanine yielded an assembly (Zn<sub>8</sub>:<sup>A104</sup>AB<sub>3</sub><sub>4</sub>) that displayed appreciable catalytic activity for the hydrolysis of *p*-nitrophenyl acetate (pNPA) ( $k_{\text{cat}} = 0.20 \text{ s}^{-1}$  and  $k_{\text{cat}}/K_{\text{m}} = 120 \text{ s}^{-1} \text{ M}^{-1}$ ) as well as the β-lactam antibiotic ampicillin ( $k_2 = 115 \text{ min}^{-1} \text{ M}^{-1}$ ) (Figure 11a). Motivated by above observations, the researchers next demonstrated that Zn<sub>8</sub>:<sup>A104</sup>AB<sub>3</sub><sub>4</sub> could properly form in the periplasm of *E. coli* cells, a remarkable feature considering that this requires selective Zn<sup>II</sup> binding and proper protein self-assembly in a highly competitive and complex environment. What is more, bacterial cells with intact Zn<sub>8</sub>:<sup>A104</sup>AB<sub>3</sub><sub>4</sub> could grow in the presence of low levels of ampicillin in the growth medium, indicating that the catalytic activity of this artificial metalloenzyme conferred the benefit of survival (Figure

11a) [73]. With this built-in selection system,  $A^{104}AB3$  was subjected to directed evolution through saturation mutagenesis of residues surrounding the catalytic Zn sites. A single point mutation (E57G) gave rise to the highest rate of survival as well as the highest corresponding *in vitro*  $\beta$ -lactamase activity, with the resulting variant  $Zn_8^{G57/A104}AB3_4$  now displaying Michaelis–Menten kinetic behaviour ( $k_{cat} = 3.5 \text{ min}^{-1}$ ,  $k_{cat}/K_m = 350 \text{ min}^{-1} \text{ M}^{-1}$ ) and a catalytic proficiency [ $(k_{cat}/K_m)/k_{uncat}$ ] of 2300000 for ampicillin hydrolysis. The crystal structure of  $Zn_8^{G57/A104}AB3_4$  revealed that E57G led to the mobilization of an otherwise well-ordered loop that opens up sufficient room for substrate binding and stabilizes ampicillin interactions through its exposed hydrophobic interior. Strikingly, highly mobile loops near the catalytic sites are a key conserved feature of natural  $\beta$ -lactamases [74,75], which emerged as an unplanned consequence of *in vivo* screening (Figure 11b) [73].  $Zn_8^{G57/A104}AB3_4$  represents the first *de novo* designed protein with an *in vivo* enzymatic function and showcases the power of the strategy of combining rational, metal-directed protein self-assembly with directed evolution.

## Conclusion and outlook

Fuelled by technical advances on several fronts, our understanding and discovery of natural metalloproteins have immensely progressed over the last decade. Yet, as we attempted to illustrate in this essay, the scope of bioinorganic chemistry is far from limited to metalloproteins that natural evolution has produced. The recent studies highlighted here have established new frontiers between bioinorganic chemistry and synthetic biology, supramolecular chemistry, materials chemistry and biotechnology. Through rational protein design and engineering, bioinorganic chemists have gained access to ‘biologically unavailable’ parts of the periodic table, expanded the functions and physico-chemical attributes of metalloproteins beyond the evolutionary boundaries and created supramolecular protein architectures with unprecedented structural and materials’ properties. Excitingly, some of these new metalloprotein structures and functions can even be incorporated into living systems. Of course, the studies highlighted mainly provide proofs of principle and there is still quite a bit of ground to cover in order to reach the sophistication of naturally evolved bioinorganic systems. For example, the examples of repurposed protein interiors are based on the realization and optimization of well-established catalytic transformations in the context of protein scaffolds that were chosen for practical reasons; colloquially speaking, the systems are ‘loaded’ for a known and desired reactivity pattern. It will be a great step forward when completely new (i.e. biologically and synthetically unprecedented) classes of reactions and complex (i.e. coupled or multistep) processes can be executed by entirely novel inorganic active sites and protein scaffolds. Likewise, the protein scaffolds used as building blocks to repurpose protein exteriors were also chosen based on practical advantages like high stability/solubility and inherent symmetry and the resultant materials are compositionally simple in that they are all homomers. One of the obvious next steps will be to increase both the structural and functional complexity of such supramolecular architectures. All of these tasks will require the advent of new chemical and biochemical strategies for protein design and engineering, significant improvements in the characterization and computational/predictive modelling of protein structures as well as of the inorganic centres within such large and dynamic architectures and last but not the least, new synthetic biological strategies to seamlessly integrate the artificial bioinorganic systems into the life cycles of bacteria for their directed and ‘undirected’ evolution.

## Summary

- The rich interplay between protein scaffolds and metal ions enables metalloproteins to carry out a vast array of biological functions, but the scope of this interplay is limited to biologically available components and contexts.
- Protein engineers have repurposed existing proteins to build new metalloprotein structures and functions that lie outside the scope of natural evolution.
- Protein interiors can be repurposed to give proteins with expanded or non-biological metal-based functions without having to design a protein scaffold from scratch.
- Protein exteriors can be repurposed to create discrete supramolecular assemblies or infinite arrays with new structures and emergent functional/physical properties.

## Acknowledgements

We thank Jake Bailey for his assistance in constructing Figure 9 and many past and present colleagues in the Tezcan Lab for their contributions to the work described in the section "Repurposing protein exteriors for the metal-directed self-assembly of functional metalloprotein architectures".

## Funding

This work was supported by the National Science Foundation [grant number CHE-1306646, CHE-1607145, and DMR-1602537]; the Department of Energy [grant number DE-FG02-10ER46677]; and the Molecular Biophysics Training Grant through the National Institute of Health [grant number 5T32GM008326].

## Competing interests

The authors declare that there are no competing interests associated with the manuscript.

## Abbreviations

APX, ascorbate peroxidase; APX2, engineered APX; CYP, cytochrome P450; cyt *cb*<sub>562</sub>, cytochrome *cb*<sub>562</sub>; ee, enantiomeric excess;  $E^{\circ}_{\text{red}}$ , reduction potential; iPrOH, propan-2-ol; Ir-PPIX, protoporphyrin IX containing an Ir-methyl centre; MeTIR, metal-templated interface redesign; NMH, *N*-methylhistidine; RCM, ring-closing metathesis; Sav, streptavidin; SUP, super uranyl-binding protein; THF, tetrahydrofuran; TTN, total turnover number.

## References

- Lippard, S. and Berg, J. (1994) *Principles of Bioinorganic Chemistry*, 1st ed., University Science Books, Mill Valley
- Bertini, I., Gray, H.B., Stiefel, E.I. and Valentine, J.S. (2007) *Biological Inorganic Chemistry, Structure & Reactivity*, 1st ed., University Science Books, Sausalito
- Frausto da Silva, J.J.R. and Williams, R.J.P. (2001) *The Biological Chemistry of the Elements*, 2nd ed., Oxford University Press, Oxford
- Holm, R.H., Kennepohl, P. and Solomon, E.I. (1996) Structural and functional aspects of metal sites in biology. *Chem. Rev.* **96**, 2239–2314
- Yu, F., Cangelosi, V.M., Zastrow, M.L., Tegoni, M., Plegaria, J.S., Tebo, A.G. et al. (2014) Protein design: toward functional metalloenzymes. *Chem. Rev.* **114**, 3495–3578
- Nastri, F., Chino, M., Maglio, O., Bhagi-Damodaran, A., Lu, Y. and Lombardi, A. (2016) Design and engineering of artificial oxygen-activating metalloenzymes. *Chem. Soc. Rev.* **45**, 5020–5054
- Petrik, I.D., Liu, J. and Lu, Y. (2014) Metalloenzyme design and engineering through strategic modifications of native protein scaffolds. *Curr. Opin. Chem. Biol.* **19**, 67–75
- Harding, M.M., Nowicki, M.W. and Walkinshaw, M.D. (2010) Metals in protein structures: a review of their principal features. *Crystallogr. Rev.* **16**, 247–302
- Song, W.J., Sontz, P.A., Ambroggio, X.I. and Tezcan, F.A. (2014) Metals in protein-protein interfaces. *Annu. Rev. Biophys.* **43**, 409–431
- Waldron, K.J., Rutherford, J.C., Ford, D. and Robinson, N.J. (2009) Metalloproteins and metal sensing. *Nature* **460**, 823–830
- Williams, R.J.P. (1991) The chemical elements of life. *J. Chem. Soc., Dalton Trans.* 539–546
- Williams, R.J.P. (2003) Metallo-enzyme catalysis. *Chem. Commun.* 1109–1113
- Messerschmidt, A., Huber, R., Poulos, T. and Wieghardt, K. (2001) *Handbook of Metalloproteins: Vols. 1 & 2*, John Wiley Sons, Chichester
- Kendrew, J.C., Bodo, G., Dintzis, H.M., Parrish, R.G., Wyckoff, H. and Phillips, D.C. (1958) A three-dimensional model of the myoglobin molecule obtained by X-ray analysis. *Nature* **181**, 662–666
- Perutz, M.F., Rossmann, M.G., Cullis, A.F., Muirhead, H., Will, G. and North, A.C.T. (1960) Structure of haemoglobin: a three-dimensional Fourier synthesis at 5.5-Å resolution, obtained by X-ray analysis. *Nature* **185**, 416–422
- Li, S., Ahmed, L., Zhang, R., Pan, Y., Matsunami, H., Burger, J.L. et al. (2016) Smelling sulfur: copper and silver regulate the response of human odorant receptor OR2T11 to low-molecular-weight thiols. *J. Am. Chem. Soc.* **138**, 13281–13288
- Wagner, T., Ermler, U. and Shima, S. (2016) The methanogenic CO<sub>2</sub> reducing-and-fixing enzyme is bifunctional and contains 46 [4Fe-4S] clusters. *Science* **354**, 114–117
- Gu, J., Wu, M., Guo, R., Yan, K., Lei, J., Gao, N. et al. (2016) The architecture of the mammalian respirasome. *Nature* **537**, 639–643
- Salgado, E.N., Radford, R.J. and Tezcan, F.A. (2010) Metal-directed protein self-assembly. *Acc. Chem. Res.* **43**, 661–672
- Radford, R.J., Brodin, J.D., Salgado, E.N. and Tezcan, F.A. (2011) Expanding the utility of proteins as platforms for coordination chemistry. *Coord. Chem. Rev.* **255**, 790–803
- Martell, J.D., Deerinck, T.J., Sancak, Y., Poulos, T.L., Mootha, V.K., Sosinsky, G.E. et al. (2012) Engineered ascorbate peroxidase as a genetically encoded reporter for electron microscopy. *Nat. Biotechnol.* **30**, 1143–1148
- Srivastava, P., Yang, H., Ellis-Guardiola, K. and Lewis, J.C. (2015) Engineering a dirhodium artificial metalloenzyme for selective olefin cyclopropanation. *Nat. Commun.* **6**, 7789
- Khare, S.D., Kipnis, Y., Greisen, Jr, P., Takeuchi, R., Ashani, Y., Goldsmith, M. et al. (2012) Computational redesign of a mononuclear zinc metalloenzyme for organophosphate hydrolysis. *Nat. Chem. Biol.* **8**, 294–300



- 24 Savile, C.K., Janey, J.M., Mundorff, E.C., Moore, J.C., Tam, S., Jarvis, W.R. et al. (2010) Biocatalytic asymmetric synthesis of chiral amines from ketones applied to sitagliptin manufacture. *Science* **329**, 305–309
- 25 Reynolds, E.W., McHenry, M.W., Cannac, F., Gober, J.G., Snow, C.D. and Brustad, E.M. (2016) An evolved orthogonal enzyme/cofactor pair. *J. Am. Chem. Soc.* **138**, 12451–12458
- 26 Tyagi, V. and Fasan, R. (2016) Myoglobin-catalyzed olefination of aldehydes. *Angew. Chem. Int. Ed. (English)* **55**, 2512–2516
- 27 Kolodny, R., Pereyaslavets, L., Samson, A.O. and Levitt, M. (2013) On the universe of protein folds. *Annu. Rev. Biophys.* **42**, 559–582
- 28 Ingles-Prieto, A., Ibarra-Molero, B., Delgado-Delgado, A., Perez-Jimenez, R., Fernandez, J.M., Gaucher, E.A. et al. (2013) Conservation of protein structure over four billion years. *Structure* **21**, 1690–1697
- 29 Rulek, L. and Vondráček, J. (1998) Coordination geometries of selected transition metal ions ( $\text{Co}^{2+}$ ,  $\text{Ni}^{2+}$ ,  $\text{Cu}^{2+}$ ,  $\text{Zn}^{2+}$ ,  $\text{Cd}^{2+}$ , and  $\text{Hg}^{2+}$ ) in metalloproteins. *J. Inorg. Biochem.* **71**, 115–127
- 30 Pible, O., Guilbaud, P., Pellequer, J.L., Vidaud, C. and Quemener, E. (2006) Structural insights into protein-uranyl interaction: towards an in silico detection method. *Biochimie* **88**, 1631–1638
- 31 Zhou, L., Bosscher, M., Zhang, C., Özçubukçu, S., Zhang, L., Zhang, W. et al. (2014) A protein engineered to bind uranyl selectively and with femtomolar affinity. *Nat. Chem.* **6**, 236–241
- 32 Liu, J., Chakraborty, S., Hosseinzadeh, P., Yu, Y., Tian, S., Petrik, I. et al. (2014) Metalloproteins containing cytochrome, iron–sulfur, or copper redox centers. *Chem. Rev.* **114**, 4366–4469
- 33 Marshall, N.M., Garner, D.K., Wilson, T.D., Gao, Y.-G., Robinson, H., Nilges, M.J. et al. (2009) Rationally tuning the reduction potential of a single cupredoxin beyond the natural range. *Nature* **462**, 113–116
- 34 Hosseinzadeh, P., Marshall, N.M., Chacon, K.N., Yu, Y., Nilges, M.J., New, S.Y. et al. (2016) Design of a single protein that spans the entire 2-V range of physiological redox potentials. *Proc. Natl. Acad. Sci. U.S.A.* **113**, 262–267
- 35 Green, A.P., Hayashi, T., Mittl, P.R.E. and Hilvert, D. (2016) A chemically programmed proximal ligand enhances the catalytic properties of a heme enzyme. *J. Am. Chem. Soc.* **138**, 11344–11352
- 36 Poulos, T.L. (1996) The role of the proximal ligand in heme enzymes. *J. Biol. Inorg. Chem.* **1**, 356–359
- 37 Goodin, D.B. (1996) When an amide is more like histidine than imidazole: the role of axial ligands in heme catalysis. *J. Biol. Inorg. Chem.* **1**, 360–363
- 38 Jäckel, C., Kast, P. and Hilvert, D. (2008) Protein design by directed evolution. *Annu. Rev. Biophys.* **37**, 153–173
- 39 Romero, P.A. and Arnold, F.H. (2009) Exploring protein fitness landscapes by directed evolution. *Nat. Rev. Mol. Cell Biol.* **10**, 866–876
- 40 Reetz, M.T. (2011) Laboratory evolution of stereoselective enzymes: a prolific source of catalysts for asymmetric reactions. *Angew. Chem. Int. Ed. (English)* **50**, 138–174
- 41 Coelho, P.S., Brustad, E.M., Kannan, A. and Arnold, F.H. (2013) Olefin cyclopropanation via carbene transfer catalyzed by engineered cytochrome P450 enzymes. *Science* **339**, 307–310
- 42 Coelho, P.S., Wang, Z.J., Ener, M.E., Baril, S.A., Kannan, A., Arnold, F.H. et al. (2013) A serine-substituted P450 catalyzes highly efficient carbene transfer to olefins *in vivo*. *Nat. Chem. Biol.* **9**, 485–487
- 43 Farwell, C.C., Zhang, R.K., McIntosh, J.A., Hyster, T.K. and Arnold, F.H. (2015) Enantioselective enzyme-catalyzed aziridination enabled by active-site evolution of a cytochrome P450. *ACS Cent. Sci.* **1**, 89–93
- 44 Kan, S.B., Lewis, R.D., Chen, K. and Arnold, F.H. (2016) Directed evolution of cytochrome c for carbon–silicon bond formation: binging silicon to life. *Science* **354**, 1048–1051
- 45 Wilson, M.E. and Whitesides, G.M. (1978) Conversion of a protein to a homogeneous asymmetric hydrogenation catalyst by site-specific modification with a diphosphinerhodium(II) moiety. *J. Am. Chem. Soc.* **100**, 306–307
- 46 Yamamura, K. and Kaiser, E.T. (1976) Studies on the oxidase activity of copper(II) carboxypeptidase A. *J. Chem. Soc., Chem. Commun.* 830–831
- 47 Chan, K.-H., Guan, X., Lo, V.K.-Y. and Che, C.-M. (2014) Elevated catalytic activity of ruthenium(II)–porphyrin-catalyzed carbene/nitrene transfer and insertion reactions with N-heterocyclic carbene ligands. *Angew. Chem. Int. Ed. (English)* **53**, 2982–2987
- 48 Maxwell, J.L., O'Malley, S., Brown, K.C. and Kodadek, T. (1992) Shape-selective and asymmetric cyclopropanation of alkenes catalyzed by rhodium porphyrins. *Organometallics* **11**, 645–652
- 49 Anding, B.J., Ellern, A. and Woo, L.K. (2012) Olefin cyclopropanation catalyzed by iridium(III) porphyrin complexes. *Organometallics* **31**, 3628–3635
- 50 Key, H.M., Dydio, P., Clark, D.S. and Hartwig, J.F. (2016) Abiological catalysis by artificial haem proteins containing noble metals in place of iron. *Nature* **534**, 534–537
- 51 Dydio, P., Key, H.M., Nazarenko, A., Rha, J.Y.-E., Seyedkazemi, V., Clark, D.S. et al. (2016) An artificial metalloenzyme with the kinetics of native enzymes. *Angew. Chem. Int. Ed. (English)* **354**, 102–106
- 52 Heinisch, T. and Ward, T.R. (2016) Artificial metalloenzymes based on the biotin–streptavidin technology: challenges and opportunities. *Acc. Chem. Res.* **49**, 1711–1721
- 53 Creus, M., Pordea, A., Rossel, T., Sardo, A., Letondor, C., Ivanova, A. et al. (2008) X-ray structure and designed evolution of an artificial transfer hydrogenase. *Angew. Chem. Int. Ed. (English)* **47**, 1400–1404
- 54 Heinisch, T., Langowska, K., Tanner, P., Reymond, J.-L., Meier, W., Palivan, C. et al. (2013) Fluorescence-based assay for the optimization of the activity of artificial transfer hydrogenase within a biocompatible compartment. *Chem. Cat. Chem.* **5**, 720–723
- 55 Chatterjee, A., Mallin, H., Klehr, J., Vallapurackal, J., Finke, A.D., Vera, L. et al. (2016) An enantioselective artificial Suzukiase based on the biotin–streptavidin technology. *Chem. Sci.* **7**, 673–677
- 56 Hyster, T.K., Knorr, L., Ward, T.R. and Rovis, T. (2012) Biotinylated Rh(III) complexes in engineered streptavidin for accelerated asymmetric C–H activation. *Science* **338**, 500–503
- 57 Jeschek, M., Reuter, R., Heinisch, T., Trindler, C., Klehr, J., Panke, S. et al. (2016) Directed evolution of artificial metalloenzymes for *in vivo* metathesis. *Nature* **537**, 661–665

- 58 Goodsell, D.S. and Olson, A.J. (2000) Structural symmetry and protein function. *Annu. Rev. Biophys. Struct.* **29**, 105–153
- 59 Alberts, B. and Miake-Lye, R. (1992) Unscrambling the puzzle of biological machines: the importance of the details. *Cell* **68**, 415–420
- 60 Salgado, E.N., Faraone-Mennella, J. and Tezcan, F.A. (2007) Controlling protein-protein interactions through metal coordination: assembly of a 16-helix bundle protein. *J. Am. Chem. Soc.* **129**, 13374–13375
- 61 Radford, R.J. and Tezcan, F.A. (2009) A superprotein triangle driven by nickel(II) coordination: exploiting non-natural metal ligands in protein self-assembly. *J. Am. Chem. Soc.* **131**, 9136–9137
- 62 Salgado, E.N., Lewis, R.A., Mossin, S., Rheingold, A.L. and Tezcan, F.A. (2009) Control of protein oligomerization symmetry by metal coordination: C<sub>2</sub> and C<sub>3</sub> symmetrical assemblies through Cu(II) and Ni(II) coordination. *Inorg. Chem.* **48**, 2726–2728
- 63 Padilla, J.E., Colovos, C. and Yeates, T.O. (2001) Nanohedra: using symmetry to design self assembling protein cages, layers, crystals, and filaments. *Proc. Natl. Acad. Sci. U.S.A.* **98**, 2217–2221
- 64 Brodin, J.D., Ambroggio, X.I., Tang, C.Y., Parent, K.N., Baker, T.S. and Tezcan, F.A. (2012) Metal-directed, chemically tunable assembly of one-, two- and three-dimensional crystalline protein arrays. *Nat. Chem.* **4**, 375–382
- 65 Brodin, J.D., Smith, S.J., Carr, J.R. and Tezcan, F.A. (2015) Designed, helical protein nanotubes with variable diameters from a single building block. *J. Am. Chem. Soc.* **137**, 10468–10471
- 66 Guthold, M., Liu, W., Sparks, E.A., Jawerth, L.M., Peng, L., Falvo, M. et al. (2007) A comparison of the mechanical and structural properties of fibrin fibers with other protein fibers. *Cell Biochem. Biophys.* **49**, 165–181
- 67 Suzuki, Y., Cardone, G., Restrepo, D., Zavattieri, P.D., Baker, T.S. and Tezcan, F.A. (2016) Self-assembly of coherently dynamic, auxetic, two-dimensional protein crystals. *Nature* **533**, 369–373
- 68 Sontz, P.A., Bailey, J.B., Ahn, S. and Tezcan, F.A. (2015) A metal organic framework with spherical protein nodes: rational chemical design of 3D protein crystals. *J. Am. Chem. Soc.* **137**, 11598–11601
- 69 Brodin, J.D., Carr, J.R., Sontz, P.A. and Tezcan, F.A. (2014) Exceptionally stable, redox-active supramolecular protein assemblies with emergent properties. *Proc. Natl. Acad. Sci. U.S.A.* **111**, 2897–2902
- 70 Salgado, E.N., Ambroggio, X.I., Brodin, J.D., Lewis, R.A., Kuhlman, B. and Tezcan, F.A. (2010) Metal-templated design of protein interfaces. *Proc. Natl. Acad. Sci. U.S.A.* **107**, 1827–1832
- 71 Brodin, J.D., Medina-Morales, A., Ni, T., Salgado, E.N., Ambroggio, X.I. and Tezcan, F.A. (2010) Evolution of metal selectivity in templated protein interfaces. *J. Am. Chem. Soc.* **132**, 8610–8617
- 72 Churchfield, L.A., Medina-Morales, A., Brodin, J.D., Perez, A. and Tezcan, F.A. (2016) *De novo* design of an allosteric metalloprotein assembly with strained disulfide bonds. *J. Am. Chem. Soc.* **138**, 13163–13166
- 73 Song, W.J. and Tezcan, F.A. (2014) A designed supramolecular protein assembly with *in vivo* enzymatic activity. *Science* **346**, 1525–1528
- 74 Scrofani, S.D., Chung, J., Huntley, J.J., Benkovic, S.J., Wright, P.E. and Dyson, H.J. (1999) NMR characterization of the metallo-beta-lactamase from *Bacteroides fragilis* and its interaction with a tight-binding inhibitor: role of an active-site loop. *Biochemistry* **38**, 14507–14514
- 75 Tomatis, P.E., Fabiane, S.M., Simona, F., Carloni, P., Sutton, B.J. and Vila, A.J. (2008) Adaptive protein evolution grants organismal fitness by improving catalysis and flexibility. *Proc. Natl. Acad. Sci. U.S.A.* **105**, 20605–20610